PAPER

Polyvinylpyrrolidone/cellulose acetate nanofibers synthesized using electrospinning method and their characteristics

View the article online for updates and enhancements.

Recent citations

Materials Research Express

PAPER

Polyvinylpyrrolidone/cellulose acetate nanofibers synthesized using electrospinning method and their characteristics

Jaidan Jauhari[1], **Sendi Wiranata**[1,2], **Annisa Rahma**[3], **Zainuddin Nawawi**[4] and **Ida Sriyanti**[1,2] ⓘD

1   Laboratory of Instrumentation and Nanotechnology Applications, Faculty of Computer Science, Universitas Sriwijaya, Palembang, Indonesia
2   Department of Physics Education, Faculty of Education, Universitas Sriwijaya, Palembang, Indonesia
3   Pharmaceutics Department, Institut Teknologi Bandung, Bandung, Indonesia
4   Department of Electrical Engineering, Universitas Sriwijaya, Palembang, Indonesia

E-mail: ida_sriyanti@unsri.ac.id

Abstract

Polyvinylpyrrolidone (PVP) is among the most extensively used polymer in electrospinning. It has excellent electrospinnabibilty, aqueous solubility, and biocompatibility. PVP has demonstrated potential application as drug delivery matrix and wound dressing material. However, PVP is easily degraded in the presence of moisture/water. Incorporation of cellulose acetate (CA) in PVP nanofiber is a promising way to increase of resistance to water. The objective of this study was to prepare to PVP/CA nanofiber by electrospinning method and to determine their characteristics. The SEM result shows that electrospinning of PVP/CA solution at 5% concentration (FC1) resulted in beaded fiber. At 10% (FC2) and 15% (FC3) concentration, the resulted PVP/CA fibers were bead-free. The average diameter of FC1-, FC2-, and FC3 were 258, 398, 534 nm, respectively. The FTIR analysis confirmed the presence of PVP and CA in FC1-, FC2- and FC3 nanofiber as indicated by characteristic peaks of hydroxyl groups and cyclic amides (PVP); and alkane and carboxyl groups (CA). The XRD study revealed amorphous state of PVP nanofiber and crystallinity state of CA nanofiber. The mechanical test showed that electrospun fiber with smaller diameter had greater tensile strength. The presence of CA increased the functional properties of PVP-based nanofiber.

1. Introduction

Electrospinning technique is a method widely used in recent years. Its simplicity and rapid process allow production of polymeric fibers with diameter ranging from nanometer to micrometer scale [1, 2]. This technique involves (1) Coulomb forces resulted from the applied electrical charge and (2) elongation of the polymer solution. Upon exposure to a very high electrical potential or voltage difference, the charged polymer is attracted to the collector and forms fiber strands [3]. The morphology, size, and surface of the fibers can be customized by adjusting processing parameters such as molecular weight, polymer concentration, electric voltage, needle-collector spacing, needle shape, polymer solution flow rate, and collector geometry; or by adjusting solution parameters such as conductivity, viscosity, and surface tension [3–5]. The structure of the nanofiber can be tailored to fulfill the desired characteristics, depending on the application. Electrospun fiber has been explored for drug delivery [4, 6, 7], air filtration, tissue engineering [8] and wound healing [9, 10] purpose.

A broad range of polymers with various characteristics can be used in the sythesis of electrospun nanofiber. In this study, we used polyvinylpyrrolidone polymer (PVP). PVP was chosen because it is easily electrospun, non-toxic, and biocompatible [4, 7, 11]. In addition, PVP is often used as the matrix for active substances in pharmaceutical dosage forms. The high solubility of PVP generally results in rapid drug release [12]. Therefore, PVP needs to be combined with another polymer with lower aqueous solubility, such as cellulose acetate (CA). CA is a natural polymer belonging to the polysaccharide, derivative or acetate ester of cellulose that is present in plant cell walls [3]. Despite its limited solubility, CA is able to form electrospun nanofiber [13–16] and promote
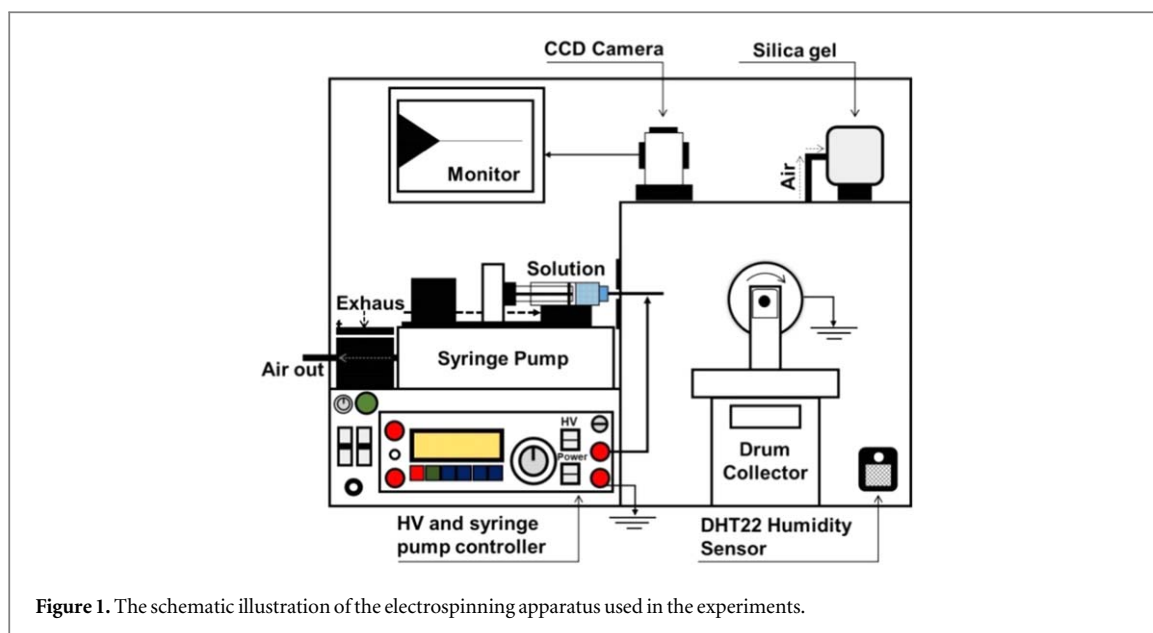
Figure 1. The schematic illustration of the electrospinning apparatus used in the experiments.

desirable drug release profile when used as a drug carrier [17, 18]. In addition, CA has a high tensile strength and elastic property. Therefore, they are widely used in a broad range of application, including wound dressing material [19, 20], drug carrier [21], filtration media [22] and supercapacitors electrode [23].

In this study, we synthesized and characterized PVP/CA nanofiber by using electrospinning technique. The morphology and structure of the FC1-, FC2- and FC3 nanofiber mats were analyzed by scanning electron microscope (SEM), x-ray Diffraction (XRD), Fourier transforms of the infrared spectrophotometer (FT-IR) and mechanical test of the nanofibers were investigated. The effect of increased PVP/CA concentrations in FC1-, FC2- and FC3 nanofibers on morphology, molecular interactions, structural changes, and nanofiber tensile strength were evaluated.

2. Experimental

The materials used to produce PVP/CA nanofiber were Polyvinypyrrolidone (PVP) (MW 130 00 00 kg mol^{-1}) and Cellulose Acetate (CA) (Mw 50 000 kg mol^{-1}) obtained from Sigma Aldrich. Acetic acid and water are obtained from Bratachem, Bandung Indonesia. Other chemical substances used for this study were of analytical grade.

The fabrication of PVP/CA fiber started with dissolving PVP and CA at a mass ratio of 7:3 into acetic acid-water (8:2). A series of polymer concentration was prepared: 5%, 10%, and 15% (w/v), which then labeled as FC1-, FC2- and FC3, respectively.

The polymer solution was electrospun using Electrospinning apparatus (Nachriebe 600) as illustrated in schematic diagram in figure 1. The apparatus consists of a high voltage power supply, syringe with needle diameter of 0.8 mm, syringe pump, and aluminium-coated rotating collector. The apparatus was placed on a temperature- and humidity-controlled chamber (25 $\pm$ 0.5 °C, RH 50%). Initially, the polymer solution was loaded into the syringe. The polymer was then dispensed by the syringe pump at a constant flowrate of 1 ml hr^{-1}. The needle tip was positively charged at 15 kV to attract the polymer solution out of the needle. The grounded drum collector was allowed to collect the resulted fiber at rotation speed of 200 rpm and tip-collector distance of 11.0 cm. The Taylor Cone formation on the needle tip was monitored using a charge-coupled device (CCD) camera.

The morphology of FC1-, FC2- and FC3 nanofibers were determined using a scanning electron microscope (SEM, JSM-6510; JEOL, Tokyo, Japan). The size distribution of the FC1-, FC2- and FC3 fibers were determined using Origin ver.8 software (OriginLab Corporation, USA). The functional groups and changes occurring in FC1-, FC2- and FC3 nanofibers were identified using a Fourier Transform Infrared Spectroscopy (FTIR) spectrum (Alpha; Bruker, Germany) at 500–4000 cm^{-1} spectral range. The XRD patterns of PVP, CA, FC1-, FC2- and FC3 nanofiber were determined using an x-ray diffractometer (D8 Advance, Bruker). The tensile strength of FC1-, FC2- and FC3 nanofiber were determined using (Textechno H. Stein GmbH & Co. KG; Germany) with the grab and strip test method. All samples were trimmed into 3 $\times$ 20 mm rectangle with similar thickness and clamped on both sides of the apparatus and then stretched at elongation rate of 20 mm min^{-1}.
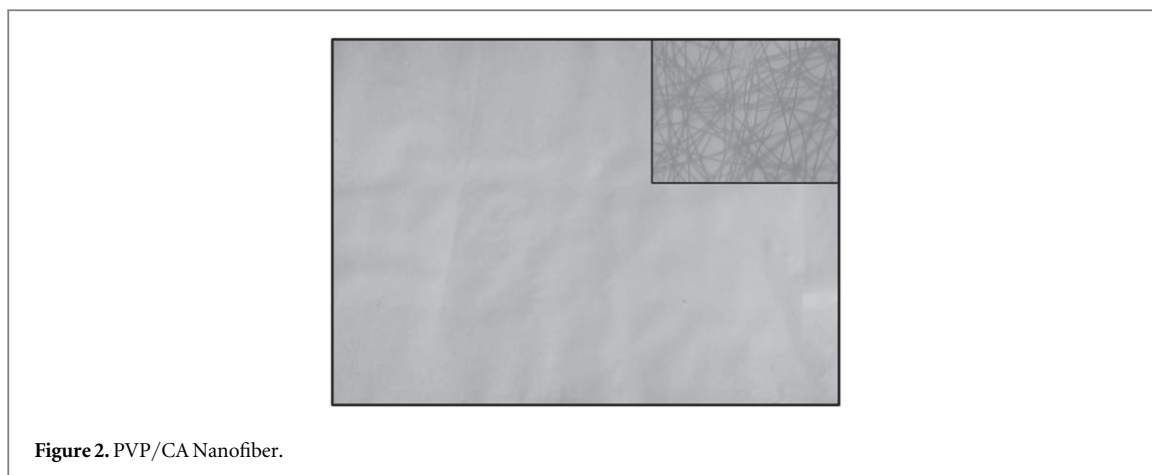
Figure 2. PVP/CA Nanofiber.
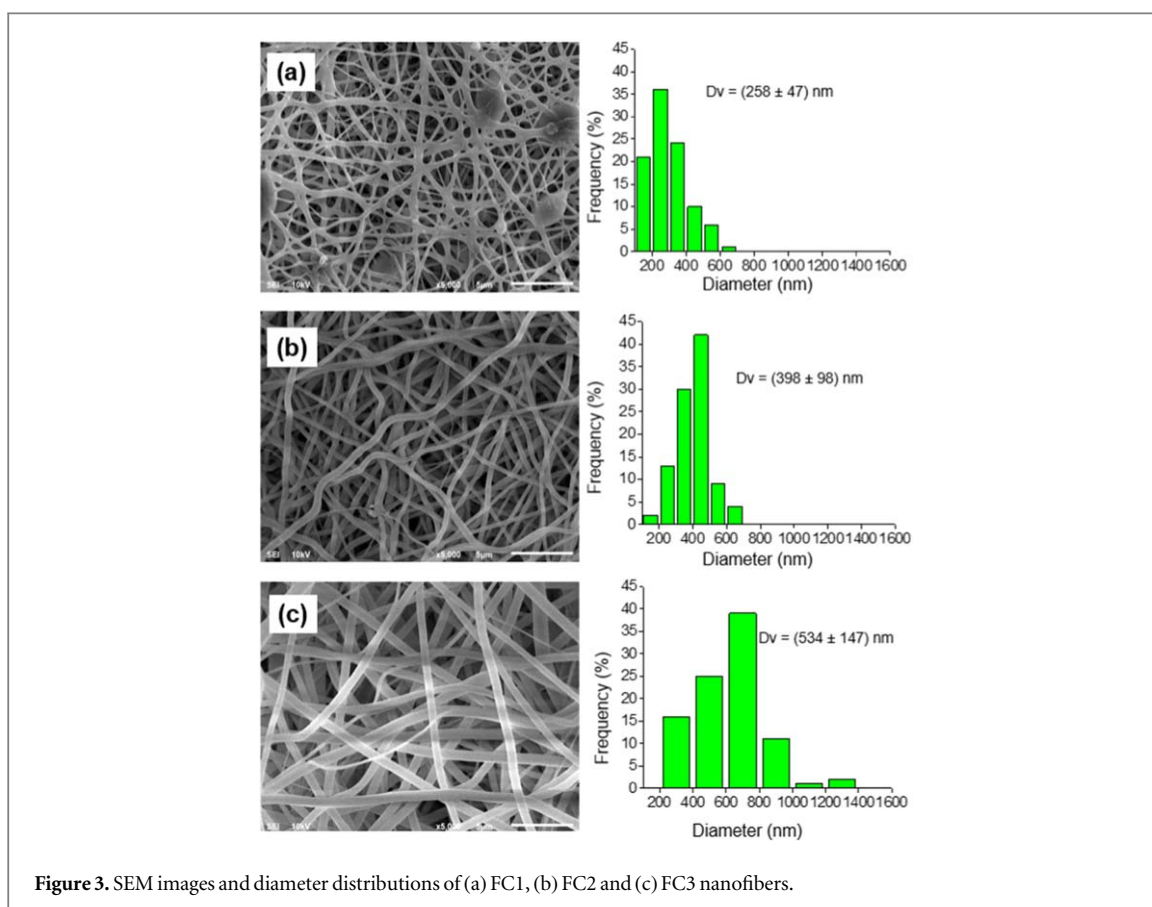
Figure 3. SEM images and diameter distributions of (a) FC1, (b) FC2 and (c) FC3 nanofibers.

3. Results and discussion

3.1. PVP/CA Image

The physical appearance of PVP/CA fibers produced from the electrospinning process can be seen in figure 2. Macroscopically, the nanofiber mats had a non-brittle, homogenous and smooth surface. The fibers formed appeared as continuous strands. The successful formation of the fibers was a result of three contributing factors. The first factor is the Coulomb force (F_c), where high electrical voltage applied on the needle tip induces charge on polymer and consequently the polymer has a tendency to move towards the grounded collector. The second factor is the loading force (F_d) from the syringe pump, which provides polymer drop available to be spun. The third factor is the surface tension force (F_γ) at the polymer-air interface, which retains the polymer droplet on the needle tip. The equilibrium of these three forces results (equation (1)) in a cone jet formation known as Taylor's cone [3].

$$F_c + F_d - F_\gamma = 0 \tag{1}$$
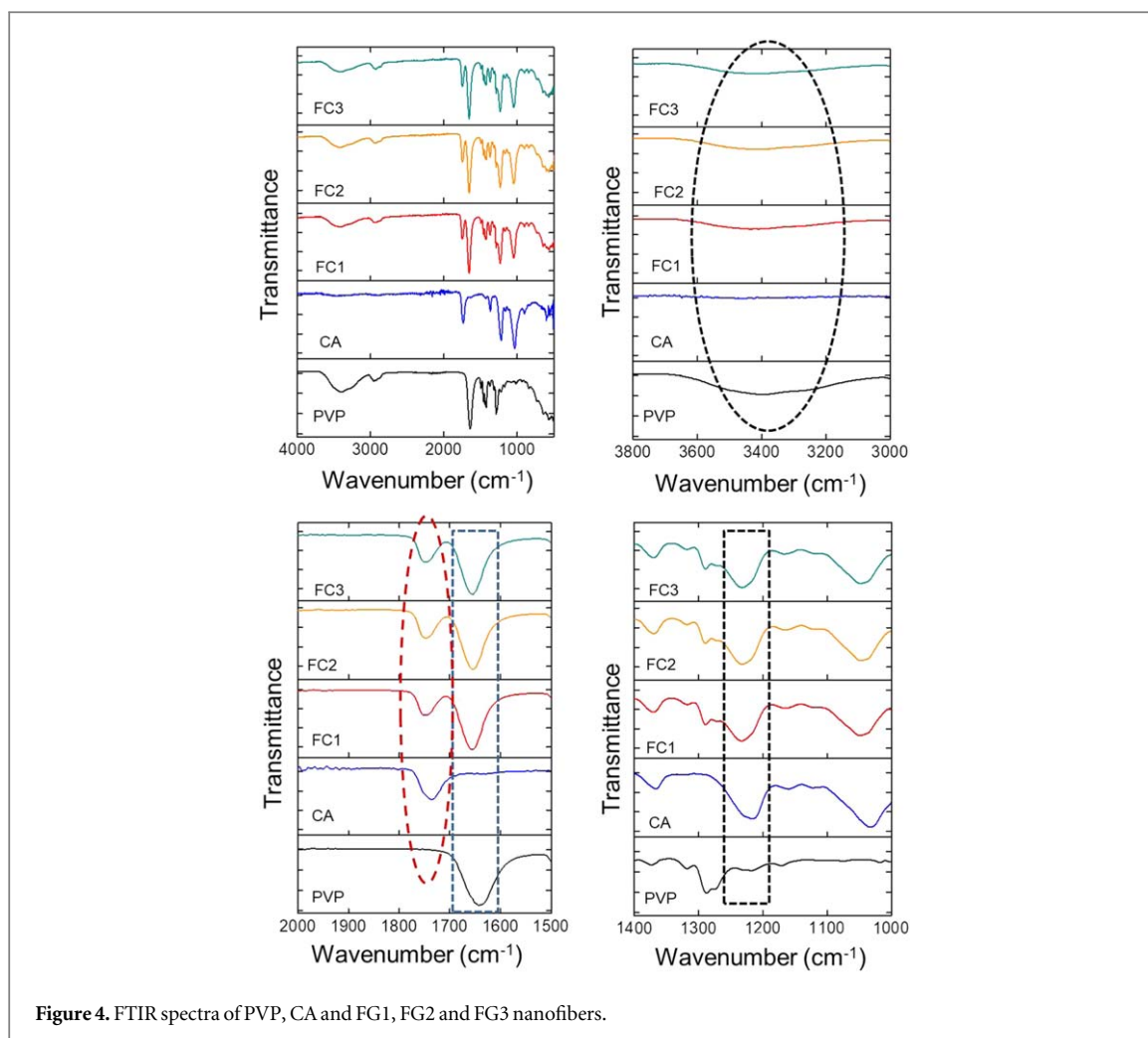
Figure 4. FTIR spectra of PVP, CA and FG1, FG2 and FG3 nanofibers.

When F_c is introduced to the polymer, the polymer chains elongates while the solvent evaporates, resulting in solidified fiber formation on the collector surface [3, 24].

3.2. Morphology and diameter of PVP/CA nanofiber

The morphology of FC1-, FC2- and FC3 fiber is shown in figure 3. Low polymer concentration (5% w/v) produced beaded fibers (figure 3(a)), which was attributed to the viscosity of the solution [25]. At low viscosity, the solution has fewer inter-chain bonds, causing the polymer solution to be unable to maintain continuous elongation during the stretching of the jet [3]. This condition will result in beaded fiber. In addition, the formation of fiber beads is related to the theory of viscoelasticity of the solution [5]. In electrospinning process, viscoelastic force permits continuous conversion of the jets into fibers instead of beads. In low viscosity solutions, the viscoelasticity of polymer droplet on the needle tip is unable to overcome Rayleigh instability, an axisymmetric rotation that causes the stretched jet to break up and form beads [5]. As the polymer concentration increases (10 and 15% w/v) bead-free fibers were produced (figures 3(b), (c)).

Increased polymer concentration affected the fiber size. In this study, the fiber diameter went up from 258 nm to 534 nm when the polymer concentration increased from 5% (w/v) to 15% (w/v). At higher concentration, more polymer chains are dispensed at specified time to be spun [26]. In addition, high polymer concentration means less solvent. Consequently, the solvent evaporates faster. This event limits the polymer elongation while accelerates polymer solidification, resulting in larger fiber formation.

3.3. FTIR analysis

FTIR study was conducted to identify characteristic functional groups in PVP, CA, FC1-, FC2- and FC3 nanofibers. The FTIR spectrum of PVP is shown in figure 4(a). The broad peak at 3380 cm^{-1} shows O–H stretching of hydroxyl groups [27]. Since PVP is a hygroscopic material, the appearance of OH-peaks in the spectrum was most probably originated from PVP interaction with moisture [28]. The other peaks indicating the presence of PVP molecules are characterized by a sharp peak at the 1656 cm^{-1}, assigned as C=O stretching of the cyclic amide group, and peaks at 1291 and 572 cm^{-1}, which indicates CN stretching and in-plane N–C=O
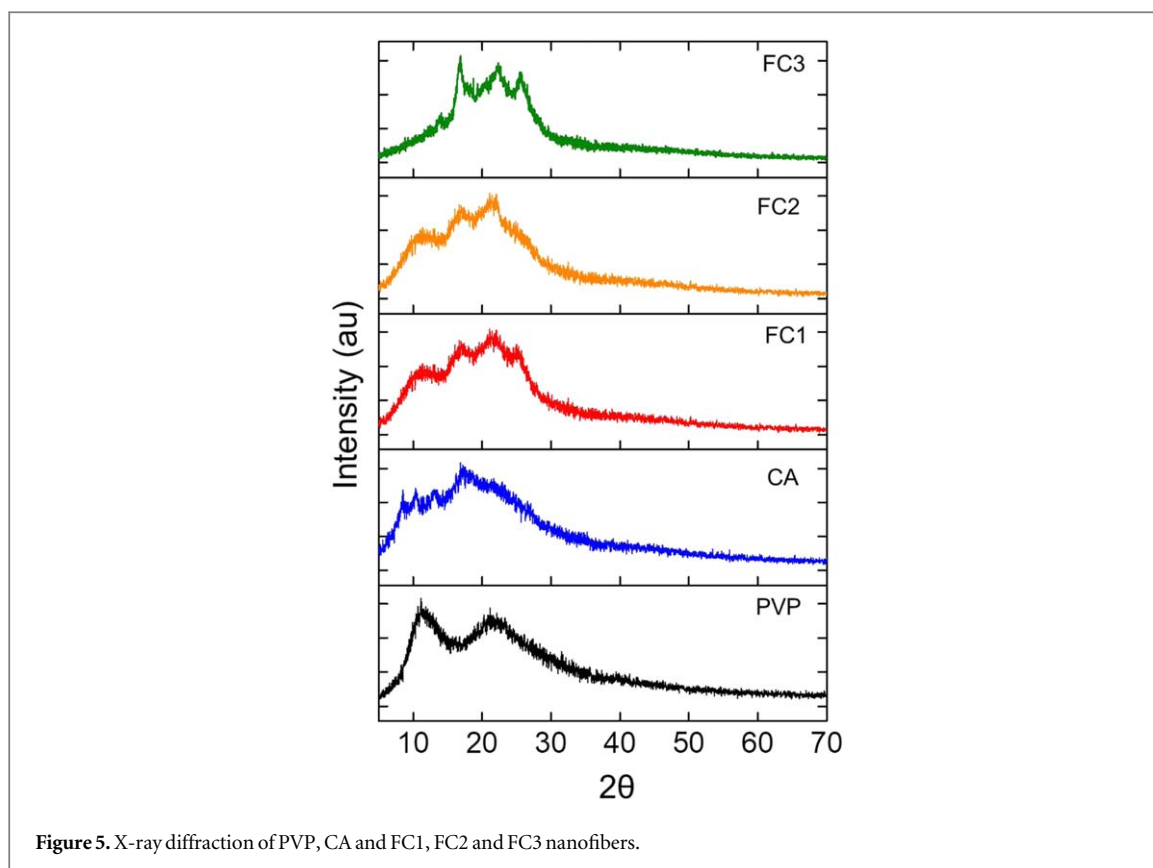
Figure 5. X-ray diffraction of PVP, CA and FC1, FC2 and FC3 nanofibers.

bending, respectively. The peak at 2953 cm^{-1} indicates CH$_2$ asymmetry bending and peak at 1440 cm^{-1} shows the deformation of C–H from the CH$_2$ group [5, 28, 29]. The FTIR spectrum of CA is shown in figure 4. The sharp peak at 1744 cm^{-1} shows C=O stretching of acetyl group and the peak at 1365 cm^{-1} shows CH rock vibration. The peak at 1221 and 1039 cm^{-1} are the characteristics of carboxyl acid groups [30, 31].

The mixing of PVP and CA produces typical peaks of PVP and CA in FC1-, FC2- and FC3 nanofiber. We observed four different features of the infrared spectrum of FC1-, FC2- and FC3 nanofiber in response to increasing PVP/CA concentration: (1) sharper hydroxyl peaks, (2) sharper cylic amide peaks in higher PVP/CA concentration, (3) sharper alkane peaks, and (4) sharper carboxyl peak. These features were also accompanied by peak shifts. Firstly, higher PVP/CA concentration lead to sharper hydroxyl peaks of PVP occurring around 3800–3000 cm^{-1}. This peak appeared at 3380 cm^{-1} in PVP but shifted towards higher wavenumber: to 3397, 3390 and 3386 cm^{-1} in FC1-, FC2- and FC3 nanofiber, respectively. Secondly, higher PVP/CA concentration lead to sharper cyclic amide stretching occurring around 1800–1650 cm^{-1}. The peak appeared at 1652 cm^{-1} in PVP, and shifted to 1667, 1661, 1656 cm^{-1} in FC1-, FC2- and FC3 nanofiber, respectively. Regarding the alkane peaks, increased PVP/CA concentration resulted in sharper alkane peaks (CH-rock vibration) occurring around 1850–1750 cm^{-1}. The peaks of CA appearing at 1745 cm^{-1} shifted to higher wavenumber, appearing at 1754, 1749 and 1748 cm^{-1} in FC1-, FC2- and FC3 nanofiber, respectively. Lastly, higher PVP/CA concentration caused the carboxyl acid peaks in CA appearing over 1230–1100 cm^{-1} to be sharper and more visible. The carboxylic acid-indicating peaks appearing at 1220 cm^{-1} shifted towards higher wavenumber, at 1231, 1226 and 1222 cm^{-1} in FC1-, FC2- and FC3 nanofiber fibers, respectively. The changes in FTIR peaks in FC1-, FC2- and FC3 nanofibers are considered to be the result of interactions between PVP and CA molecules.

3.4. X-ray diffraction analysis

The x-ray diffraction study was conducted to investigate electrospinning-induced crystalline changes. The diffraction pattern of PVP, CA and FC1-, FC2-, FC3 nanofiber is presented in figure 5. The diffraction pattern of PVP showed two broad diffraction peaks over the 2θ position of 5°–40°, peaking at 11° and 21°. This pattern indicates that PVP was in amorphous state [32]. In contrasts, CA nanofiber showed four sharp peaks at 8°, 10°, 13°, and 17°, indicating a fair degree of crystallinity [33, 34].

The XRD diffractogram of the FC1-, FC2- and FC3 nanofibers had a distinct pattern. FC1 nanofiber showed diffused peaks originated from PVP (11° and 21°) and CA (17° and 25°) [33, 35]. The PVP background and CA peaks were still obvious in FC2 nanofiber. These findings explain further our notion regarding the interactions

Table 1. Mechanical test of PVP, CA, and PVP/CA nanofiber.

Diameter nanofibers (nm)	Tensile strength (MPa)	Strain at break (%)	Young's modulus (MPa)
PVP	1.84 ± 0.12	2.41 ± 0.11	78.76 ± 1.73
CA	1.88 ± 0.50	2.42 ± 0.31	77.66 ± 1.01
534	2.22 ± 0.12	3.85 ± 0.21	57.79 ± 1.73
398	2.29 ± 0.50	6.58 ± 0.36	34.74 ± 1.06
258	5.88 ± 0.22	19.84 ± 0.81	29.63 ± 2.39

between PVP and CA molecules as described in the FTIR study. FC3 nanofiber exhibited a distinct CA peaks associated with [101] and [002] planes at 2θ positions of 17°, 22°, and 25° [33, 35], masking the PVP background. It was then suggested that electrospinning disrupt the crystalline state of CA in FC1 and FC2 nanofiber only. As the charged polymer travels from the needle tip towards the collector, polymer chain elongation and solvent evaporation takes place simultaneously [32]. Since the rapid evaporation process does not favor the formation of highly-ordered crystallites in both PVP and CA, polymers would exist in amorphous form. Similarly, it has been reported by Dai *et al* (2012) in pure polymer spinning that the effect of electrospinning process transformed crystalline emodin into amorphous state [36]. However, the extent of amorphization of PVP/CA fiber by electrospinning in FC3 nanofiber was limited. Since molecular orientation and crystallinity are influenced by the polymer concentration [37], higher crystallinity in FC3 nanofiber is expected.

3.5. Mechanical test of PVP/CA nanofiber
The results of mechanical test of FG1-, FG2- and FG3 nanofibers are shown in table 1. We found that fiber with smaller diameter had higher tensile strength and elongation. This is related to the degree of molecular orientation of polymer chains in the fibers. At a given polymer mass, fiber with the smaller diameter has more polymer chain oriented in parallel with each other, and thus more inter-chain bonds are formed and tensile strength grows along with the reduction of the diameter nanofiber [38, 39]. Meanwhile, the Young modulus value of the three nanofibers produced was in 45–65 MPa range, which is above the lowest limit of Young's modulus required to be a wound dressing (20 MPa) [40]. Therefore, the PVP/CA nanofiber meets the criteria as a good wound dressing.

4. Conclusion

A smooth and homogenous PVP/CA nanofiber mats have been successfully synthesized using the electrospinning method. At polymer concentration 10% (w/v) or higher, bead-free nanofiber was obtained. The FC1 nanofiber, with average diameter below 260 nm, had the highest tensile strength. Moreover, the polymer remained amorphous in FC1. This study provides an insight into enhancement of physical characteristics of hydrophilic nanofiber by the right choice of polymer blends.

Acknowledgments

ORCID iDs

Ida Sriyanti ⓘ https://orcid.org/0000-0001-8011-8866

References

[1] Castillo-Ortega M M, Nájera-Luna A, Rodríguez-Félix D E, Encinas J C, Rodríguez-Félix F, Romero J and Herrera-Franco P J 2011 *Materials Science and Engineering* C **31** 1772–8
[2] Sriyanti I, Edikresnha D, Munir M M, Rachmawati H and Khairurrijal K 2017 *Materials Science Forum* **880** 11–4
[3] Ramakrishna S, Fujihara K, Teo W E, Lim T C and dan Ma Z 2005 *An Introduction to Electrospinning and Nanofibers* (Singapore: World Scientific) 3–118

[4] Kusumah F H, Sriyanti I, Edikresnha D, Munir M M and Khairurrijal K 2016 *Materials Science Forum* **880** 95–8

[5] Sriyanti I, Edikresnha D, Rahma A, Munir M M, Rachmawati H and Khairurrijal K 2017 *Journal of Nanomaterial* **2017** 10-1

[6] Sriyanti I, Rahma A, Edikresnha D, Munir M M, Rachmawati H and Khairurrijal K 2017 2018 *International Journal of Nanomedicine* **13** 4927–41

[7] Pusporini P, Edikresnha D, Sriyanti I, Suciati T, Munir M M and Khairurrijal K 2018 *Materials Research Express* **5** 9-1

[8] Yoo H S, Kim T G and Park T G 2009 *Advanced Drug Delivery Reviews* **61** 1033–42

[9] Aruan N M, Sriyanti I, Edikresnha D, Suciati T, Munir M M and Khairurrijal K 2017 *Procedia Engineering* **170** 31–5

[10] Charernsriwilaiwat N, Rojanarata T, Ngawhirunpat T, Sukma M and Opanasopit P 2013 *International Journal of Pharmaceutics* **452** 333–43

[11] Jiang Y-N, Mo H-Y and Yu D-G 2012 *International Journal of Pharmaceutics* **438** 232–9

[12] Huang X and Brazel C S 2001 *Journal of Controlled Release* **73** 121–36

[13] Celebioglu A and Uyar T 2011 *Materials Letters* **65** 2291–4

[14] Han S O, Youk J H, Min K D, Kang Y O and Park W H 2008 *Materials Letters* **62** 759–62

[15] Konwarh R, Karak N and Misra M 2013 *Biotechnology Advances* **31** 421–37

[16] Vallejos M E, Peresin M S and Rojas O J 2012 *Journal of Polymers and the Environment* **20** 1075–83

[17] Suwantong O and Pankongadisak P 2014 *Polymer* **48** 7546–57

[18] Tungprapa S, Jangchud I and Supaphol P 2007 *Polymer* **48** 5030–41

[19] Liu X, Lin T, Gao Y, Xu Z, Huang C, Yao G, Jiang L, Tang Y and Wang X 2012 *Journal of Biomedical Materials Research Part B: Applied Biomaterials Biomater* **100B** 1556–65

[20] Tarus B, Fadel N, Al-Oufy A and El-Messiry M 2016 *Alexandria Engineering Journal* **55** 2975–84

[21] Risdian C, Nasir M, Rahma A and Rachmawati H 2015 *Journal of Nano Research* **3** 103–16

[22] Omollo E, Zhang C, Mwasiagi J I and Ncube S 2016 *Journal of Industrial Textiles* **45** 716–29

[23] Cai J, Niu H, Li Z, Du Y, Cizek P, Xie Z, Xiong H and Lin T 2015 *ACS Applied Materials & Interfaces* **7** 14946–53

[24] Andrady A L 2008 *Science and Technology of Polymer Nanofibers* (New Jersey: Wiley) 10–255

[25] Shenoy S L, Bates W D, Frisch H L and Wnek G E 2005 *Polymer* **46** 3372–84

[26] Vongsetskul T, Chantarodsakun T, Wongsomboon P, Rangkupan R and Tangboriboonrat P 2015 *Chiang Mai Journal of Science* **42** 436–42

[27] Andjani D, Sriyanti I, Fauzi A, Edikresnha D, Munir M M, Rachmawati H and Khairurrijal K 2017 *Procedia Engineering* **170** 14–8

[28] Saroj A L, Singh R K and Chandra S 2013 *Materials Science & Engineering B: Solid-State Materials for Advanced Technology* **178** 231–8

[29] Laot C M, Marand E and Oyama H T 1999 *Polymer* **40** 1095–108

[30] Kiatyongchai T, Wongsasulak S and Yoovidhya T 2014 *Journal Applied Polymer Science* 1–940167

[31] Kim C W, Kim D S, Kang S Y, Marquez M and Joo Y L 2006 *Polymer* **47** 5097–107

[32] Rahma A, Munir M M, Khairurrijal, Prasetyo A, Suendo V and Rachmawati H 2016 *Biological and Pharmaceutical Bulletin* **39** 163–73

[33] Kamal M, Abdelrazek E M, Sellow N M and Abdelghany A M 2018 *Journal of Advances in Physic* **14** 5303–11

[34] Shukla P, Bajpai A K and Bajpai R 2016 *Polymer Bulletin* **73** 2245–64

[35] Ching A S and Reyes L Q 2017 *IOP Conf. Series: Materials Science and Engineering* **205** 5-1

[36] Dai X Y, Nie W, Wang Y C, Shen Y, Li Y and Gan S J 2012 *Journal of Materials Science: Materials in Medicine* B **23** 2709–16

[37] Kołbuk D, Sajkiewicz P and Kowalewski T A 2012 *European Polymer Journal* **48** 275–83

[38] Wong S C, Baji A and Leng S 2008 *Polymer* **49** 4713–22

[39] Yao J, Bastiaansen C and Peijs T 2014 *Fibers* **2** 158–86

[40] Morgado P I, Aguiar-Ricardo A and Correia I J 2015 *Journal of Membrane Science* **490** 139–51